Quaternary Science Reviews 29 (2010) 2315–2324

Contents lists available at ScienceDirect

Quaternary Science Reviews

journal homepage: www.elsevier.com/locate/quascirev

Dating of Holocene western Canadian Arctic sediments by matching paleomagnetic secular variation to a geomagnetic field model

F. Barletta [a,b,*], G. St-Onge [a,b], J.E.T. Channell [c], A. Rochon [a,b]

[a] Institut des sciences de la mer de Rimouski (ISMER), 310 allée des Ursulines, Rimouski, QC G5L 3A1, Canada
[b] GEOTOP Research Center, C.P. 8888, Succursale Centre-ville, Montréal, QC H3C 3P8, Canada
[c] Department of Geological Sciences, University of Florida, 241 Williamson Hall, POB 112120, Gainesville, FL 32611, USA

ARTICLE INFO

Article history:
Received 18 January 2010
Received in revised form
27 May 2010
Accepted 28 May 2010

ABSTRACT

A recently recovered ~6-m long Holocene sedimentary sequence (piston Core 2004-804-650) collected from the Beaufort Sea (western Canadian Arctic) was dated by combining the paleomagnetic secular variation (PSV) and a time-varying spherical harmonic model of the geomagnetic field (CALS7k.2). A u-channel-based paleomagnetic study reveals the presence of a stable, single component of magnetization (MAD <5°) carried by low-coercivity ferrimagnetic minerals (most likely magnetite) in the pseudo-single domain grain size range. An age-depth model spanning the last ~6000 cal BP was established from nine paleomagnetic tie points obtained by comparing the magnetic declination profiles of Core 650 and the CALS7k.2 model output. In order to verify the robustness of the method, both the magnetic inclination and the relative paleointensity (RPI) records of Core 650 were then compared with western North American lacustrine and volcanic Holocene PSV records, as well as with previously published RPI records from the Beaufort and Chukchi Seas. Several common magnetic inclination features and similar millennial-scale fluctuations are detected among the records, supporting a common geomagnetic origin of the records, and implying consistency of the derived age model. These results show the potential of using both the CALS7k.2 model output and PSV of the geomagnetic field as a practical dating tool.

1. Introduction

In the last decades, an increasing number of globally distributed paleomagnetic data (archeomagnetic and lacustrine paleomagnetic data) have led to the development of a time-varying spherical harmonic model of the geomagnetic field CALS7k.2 over the last 7000 yr (Korte and Constable, 2005). In the recent years, several studies have revealed the potential use of the CALS7k.2 model to determine episodes of eastward and westward drift of the geomagnetic field (e.g., Dumberry and Finlay, 2007) as well as the evolution of the position of the geomagnetic poles during the Holocene (Korte and Mandea, 2008), thus giving new insights about the generation of the dipole field. On the other hand, little attention has been given to the practical use of paleomagnetic secular variation (PSV) computed by CALS7k.2 as a dating tool.

For instance, Holocene paleoceanographic reconstructions from the Canadian Arctic environments are difficult to obtain due to lack of robust chronologies (e.g., Hillaire-Marcel, 2008). Indeed, datable material is often rare and (or) not well preserved in the Arctic (e.g., Ledu et al., 2008; McKay et al., 2008). Moreover, the radiocarbon dating technique by acceleration mass spectrometry (AMS) is complicated due to an often poorly constrained radiocarbon reservoir effect (Darby et al., 2009), and diagenetic effects distort the paleomagnetic record over much of the central Arctic ocean (Channell and Xuan, 2009; Xuan and Channell, 2010). In this paper, we show how it is possible to overcome some of the problems associated with dating an Arctic marine sedimentary sequence collected from the Beaufort Sea (western Canadian Arctic) using PSV in conjunction with the CALS7k.2 model output and one radiocarbon date.

2. Regional setting

Piston core 2004-804-650PC (hereinafter referred as to Core 650) was raised from the Beaufort Sea on the Mackenzie Shelf area (Fig. 1; Table 1). Previous studies revealed that Holocene

* Corresponding author. Institut des sciences de la mer de Rimouski (ISMER), 310 allée des Ursulines, Rimouski, QC G5L 3A1, Canada. Tel.: +1 418 723 1986x1230; fax: +1 418 724 1842.
E-mail address: francesco.barletta@uqar.qc.ca (F. Barletta).

0277-3791/$ – see front matter © 2010 Elsevier Ltd. All rights reserved.
doi:10.1016/j.quascirev.2010.05.035

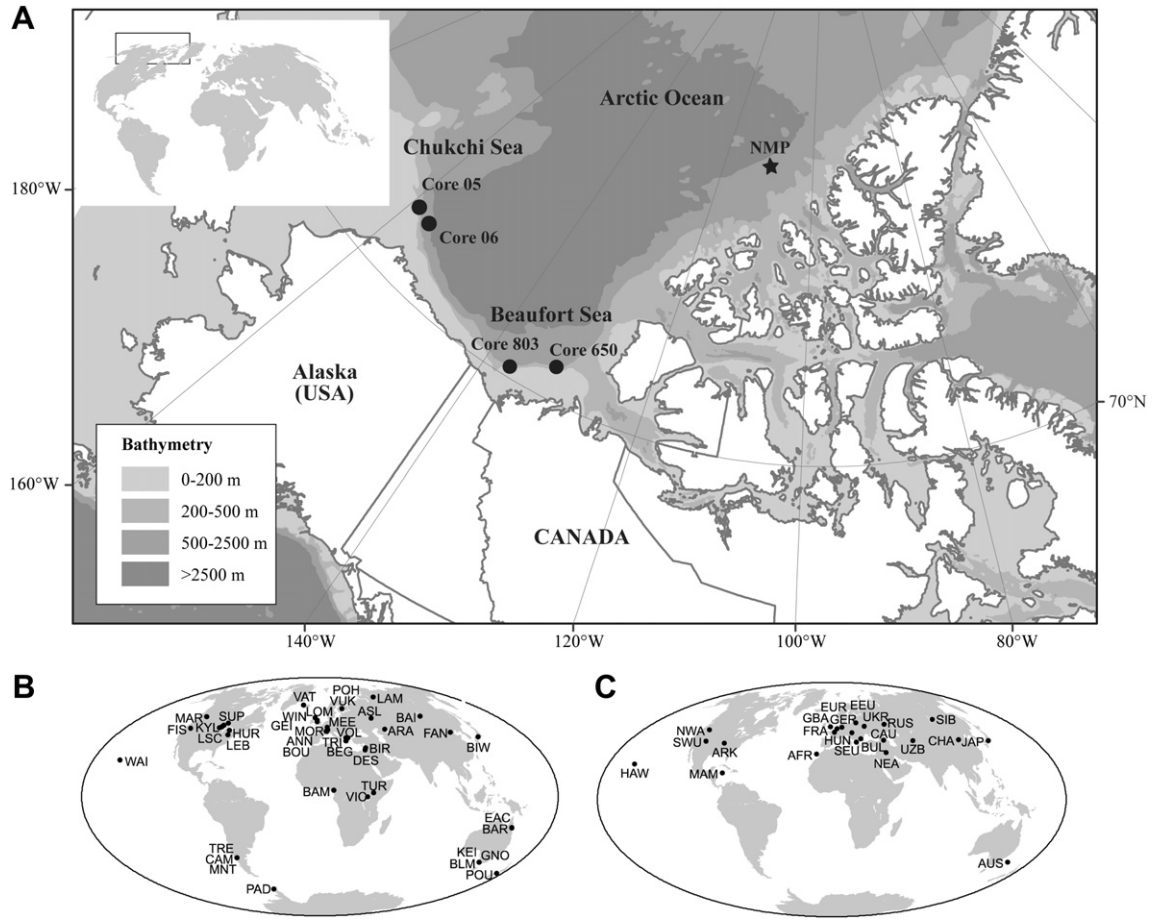

Fig. 1. (A) Location of Core 650 (this study) sampling site. Also illustrated is the location of Cores 05, 06 and 803 from the Chukchi and the Beaufort Seas (Barletta et al., 2008; Lisé-Pronovost et al., 2009). The position of the North Magnetic Pole (NMP) as determined by a joint Canada-France expedition in 2001 is indicated (Newitt et al., 2002). The box in the inset shows the location of the study area. (B) Location of the global directional paleomagnetic data compilation from sedimentary sequences and (C) from archeomagnetism used to constrain the CALS7k.2 model (modified from Korte et al., 2005). The details of the compilation are presented in Korte et al. (2005).

postglacial sedimentary sequences collected from both the Arctic Alaskan and Canadian margins are characterized by higher sedimentation rates than in the rest of the central Arctic basin (e.g., Darby et al., 2006, 2009; Rochon et al., 2006; Bringué, 2009). Holocene average sedimentation rates were estimated to vary between 10 and 300 cm/ka (e.g., Andrews and Dunhill, 2004; Keigwin et al., 2006; Rochon et al., 2006; Barletta et al., 2008; Lisé-Pronovost et al., 2009) thus offering the opportunity to reconstruct centennial- to millennial-scale geomagnetic field variations in the Arctic (e.g., Barletta et al., 2008; Lisé-Pronovost et al., 2009). Moreover, due to the proximity of the North Magnetic Pole (NMP; Fig. 1), sedimentary sequences from western Canadian Arctic have the advantage of recording higher amplitude PSV directional changes than the rest of the Earth.

Fig. 1B and C illustrate the location of the global compilation of directional paleomagnetic and archeomagnetic data, respectively, used to constrain the CALS7k.2 model (Korte et al., 2005). The directional dataset used in the CALS7k.2 model is mainly derived from lacustrine sedimentary sequences and archaeological artefacts or volcanic rocks from the Northern Hemisphere.

Table 1
Coordinates of the core.

Core	Latitude (°N)	Longitude (°W)	Water depth (m)	Length (m)
2004-804-650	71°.18.52′	131°36.98′	246	6.08

3. Materials and methods

Core 650 was collected on board the Canadian Coast Guard Icebreaker (CCGS) Amundsen during the 2004 Canadian Arctic Shelf Expedition Study (CASES). The core sections were split, described on board and then sampled with u-channel samples (u-shaped plastic liners of 2 × 2 cm cross-section and length up to 1.5 m) for paleomagnetic analyses. Apart from hysteresis properties and grain size analyses, all magnetic remanences as well as the low-field magnetic susceptibility (k_{LF}) measurements were carried out at the University of Florida (Gainesville, FL) using a 2G Enterprises Model 760R cryogenic magnetometer and a pulse magnetizer for the induction of isothermal remanent magnetizations. The continuous paleomagnetic measurements were performed at 1 cm intervals. Nonetheless, due to the response function of the magnetometer's pick-up coils each measurement integrates across a ~4.5 cm stratigraphic interval (Weeks et al., 1993). Therefore, the data from the upper and lower 4 cm of each u-channel were not used in order to eliminate edge effects (i.e., the integration of "no sediment" at the end and the beginning of each u-channel).

3.1. Magnetic measurements

U-channel samples were subjected to stepwise alternating field (AF) demagnetization of the natural remanent magnetization

Table 2
Radiocarbon date.

Core	Depth (cm)	Age[a] (yr BP)	Calibrated age[b] (cal BP)	Dated material	Lab. number[c]
2004-804-650	135	4080 ± 40	3580 (3463–3701)	*Littorina* sp.	Beta-204830

[a] The age was determined by the AMS method and corrected for natural and sputtering fractionation ($\delta^{13}C = -25‰$ versus Vienna Pee-Dee Belemnite (VPDB)). The statistical uncertainty of the age determination is given as one standard deviation (Stuiver and Polach, 1977).
[b] Calibrated using the on-line CALIB 5.0.2 software (Stuiver et al., 2005) using the Hughen et al. (2004) marine dataset. A total marine reservoir correction of ~800 yr was applied ($\Delta R = 400$ yr). The first and last ages, in parentheses, represent the 2σ cal age range.
[c] Beta analytic Inc., Miami, FL, USA.

(NRM) at peak AF fields of 0, 10–60 mT in 5 mT steps, 70 and 80 mT. In order to determine the characteristic remanent magnetization (ChRM), the magnetic declination and inclination of the ChRM (labelled as ChRM D and ChRM I, respectively) were computed at 1 cm intervals using the standard principal component analysis (PCA) of Kirschvink (1980) which also provide the maximum angular deviation (MAD) values. MAD values lower than 5° are indicative of high-quality directional data (e.g., Stoner and St-Onge, 2007). Subsequently, the stepwise acquisition and demagnetization of both the anhysteretic and isothermal remanent magnetizations (indicated as ARM and IRM, respectively) were acquired with the aim to characterize changes in magnetic mineral concentration. The ARM was imparted using a 100 mT AF field superposed to a direct current (DC) bias field of 50 μT whereas two IRMs were acquired applying a DC pulse field of 0.3 T and 0.95 T (corresponding to a saturated isothermal remanent magnetization, SIRM) respectively. These IRMs were used to construct a coercivity-dependent proxy by dividing the IRM at 0.3 T by the SIRM (St-Onge et al., 2003). This ratio is useful to estimate changes in magnetic mineralogy, with values close to 1 indicating a low-coercivity ferrimagnetic mineralogy (e.g., magnetite) and lower values indicating a higher coercivity, possibly antiferromagnetic (e.g., hematite) mineralogy.

Both the ARM and IRMs were then demagnetized at the same AF steps as the NRM. The ARM was also expressed as an anhysteretic susceptibility (k_{ARM}) by normalizing the ARM with the biasing field. AF demagnetization data were used to compute the median destructive fields of the NRM, ARM and IRM (labelled as MDF_{NRM}, MDF_{ARM}, MDF_{IRM}, respectively; i.e., the value of the peak AF necessary to reduce the magnetic remanence to half of its initial

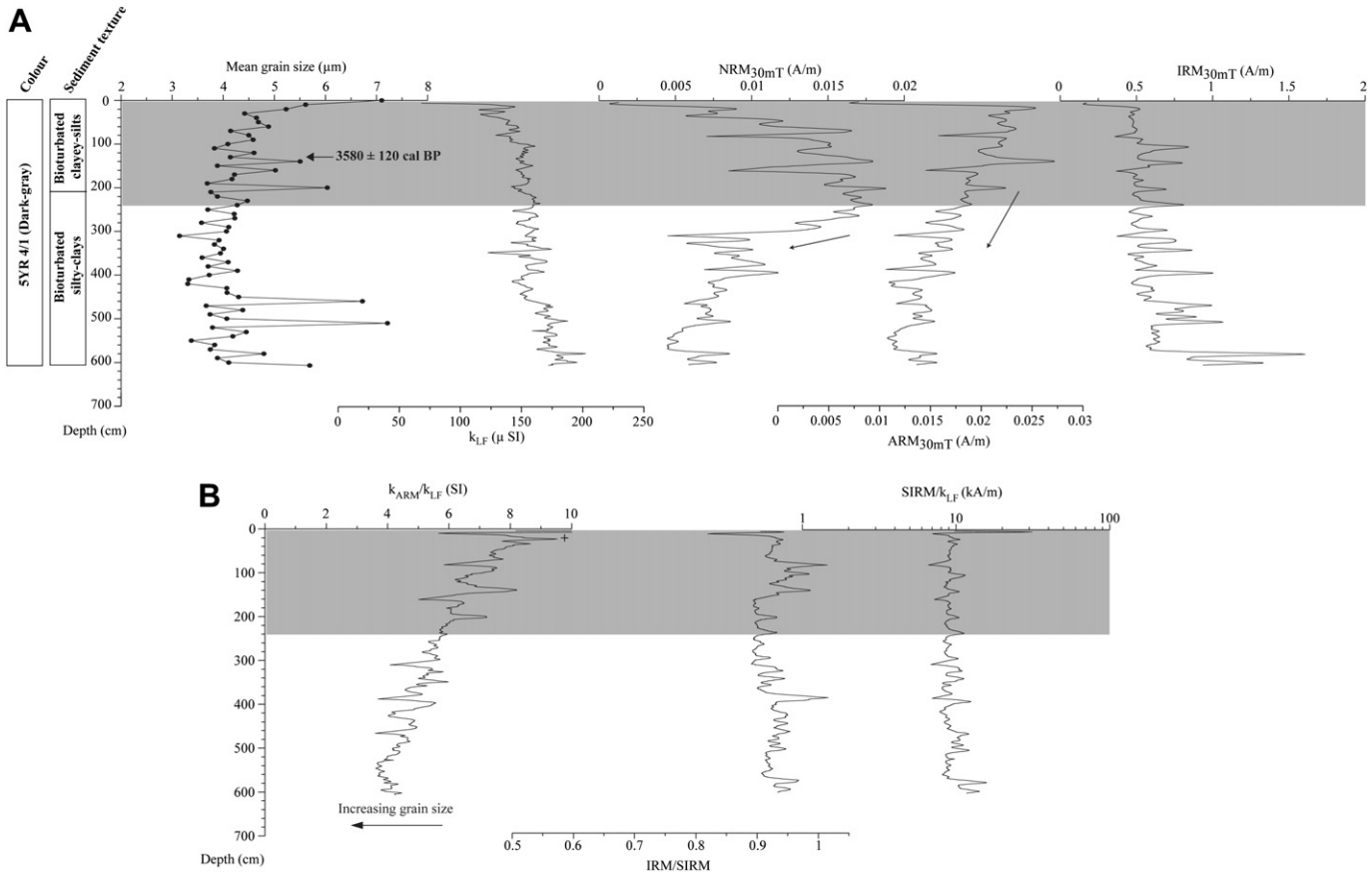

Fig. 2. Lithology and magnetic properties of Core 650. (A) Illustrated are mean grain size, low-field magnetic susceptibility (k_{LF}), natural remanent magnetization (NRM), anhysteretic remanent magnetization (ARM) and isothermal remanent magnetization (IRM) diagrams after an AF demagnetization at 30 mT. Arrows indicate decrease in remanence intensity with depth (see text for details). The only available AMS-^{14}C date is also indicated. (B) Magnetic parameters k_{ARM}/k_{LF}, IRM/SIRM and SIRM/k_{LF} against depth. The ratio IRM/SIRM is calculated after an AF demagnetization level of 30 mT in order to emphasize the relative importance of the high-coercivity component. The gray shaded area indicates the interval used for PSV and RPI reconstructions.

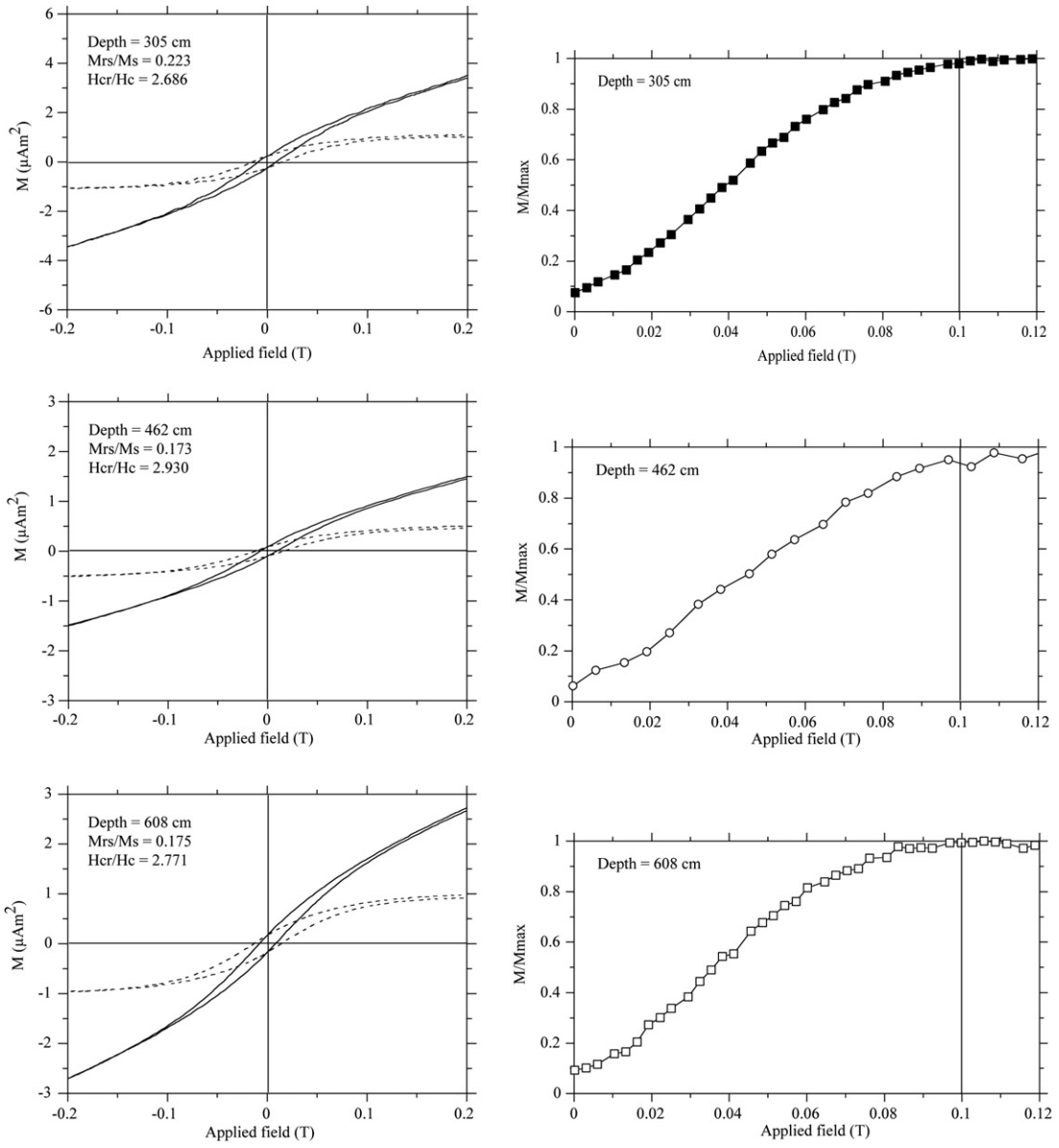

Fig. 3. (A) Representative hysteresis loops (left diagrams) with the corresponding IRM acquisition curves (right diagrams). The hysteresis parameters (saturation magnetization (M_S), saturation remanence (M_R) and coercivity (H_C)) were determined from the paramagnetic-corrected hysteresis data (broken curve in the left diagrams). Vertical line at 100 mT is for reference.

value) using the software developed by Mazaud (2005). These three parameters are useful to characterize the mean coercivity state of the ferrimagnetic minerals which in turn depends on both the magnetic mineralogy and grain size (e.g., Dunlop and Özdemir, 1997). Furthermore, the magnetic grain size was estimated using k_{ARM} versus k_{LF} diagram (King et al., 1983). The objective here is not to determine the absolute size of the magnetic grains as it was previously shown that ARM measurements vary from one laboratory to the other (Sagnotti et al., 2003), but rather to assess the extent and uniformity of the magnetic grain size distribution. Finally, a small quantity of sediment was collected every 10 cm over the top 3 m and in some selected intervals in order to study both the hysteresis properties and the IRM acquisition curves using an alternating gradient force magnetometer (AGM) (Princeton Measurement Corporation model MicroMag 2900 AGM) at the Paleomagnetism laboratory of the *Institut des sciences de la mer de Rimouski* (ISMER).

3.2. Computerized axial tomography analysis (CAT-scan)

Digital X-ray images of all u-channel samples were obtained by computerized axial tomography (CAT-scan) analysis with a 1-mm downcore resolution. The resulting gray scale images allow us to extract a tomographic intensity profile (CT numbers; e.g., St-Onge et al., 2007). CT numbers primarily reflect changes in sediment bulk density, mineralogy as well as porosity and can be also useful to detect core deformation or coring artefacts (e.g., Guyard et al., 2007; St-Onge et al., 2007).

3.3. Grain size analyses

Grain size measurements on Core 650 were made using a Beckman-Coulter laser diffraction analyzer (Model LS-13320; 0.04–2000 μm) at ISMER at 10 cm intervals. About 0.5 g of wet sediment was mixed in Calgon electrolytic solution (sodium

hexametaphosphate, 20 g/L). Subsequently, the samples were rotated for at least 3 h using an in-house rotator and then sieved (<2 mm) over the instrument prior to analysis. The statistical grain size distribution was computed using the Gradistat software (Blott and Pye, 2001) using at least two measurements.

3.4. Radiocarbon dating

One radiocarbon age was derived from a marine shell (*Littorina* sp.) using the radiocarbon accelerator mass spectrometry (AMS) technique (Table 2). The AMS-^{14}C age was then calibrated using the on-line CALIB 5.0.2 software (Stuiver et al., 2005) using the Hughen et al. (2004) marine dataset. A regional reservoir correction (ΔR) of 400 yr was applied based on the average ΔR values derived from five dates realized on pelecypod shells from the Amundsen Gulf area collected prior to atmospheric nuclear testing (McNeely et al., 2006).

4. Results

4.1. Stratigraphy

According to the visual description, Core 650 consists of bioturbated olive dark-gray (5YR 4/1) mud (Fig. 2A). As a whole, the mean grain size profile appears quite uniform (Fig. 2A). A gradual transition in sediment texture from silty-clays to clayey-silts is observed at 210 cm (Fig. 2A). The homogeneous and bioturbated sedimentary facies that characterizes the entire core and the available AMS-^{14}C date suggest that Core 650 is composed entirely of postglacial sediments. This conclusion is consistent with recent cores collected in the Beaufort and Chukchi Seas (e.g., Andrews and Dunhill, 2004; Keigwin et al., 2006; Rochon et al., 2006; Barletta et al., 2008; Lisé-Pronovost et al., 2009; Polyak et al., 2009).

4.2. Magnetic properties

Occasional black horizons and diffuse laminae are observed in the core probably due to presence of iron sulfides. However, the magnetic mineralogy-dependent ratio SIRM/k_{LF} varies between ~7 and 12 kA/m, whereas the IRM/SIRM values are close to 1 (Fig. 2B). These values are consistent with a mixed assemblage containing magnetite and titanomagnetite (Peters and Thompson, 1998; Stoner and St-Onge, 2007).

The magnetic concentration-dependent parameter ARM indicates that there is a slight decrease in remanence intensity with depth, suggesting possible downcore particle dissolution (Fig. 2A). The magnetic grain size sensitive ratio k_{ARM}/k_{LF} also displays a gradual downcore decrease suggesting a coarsening of the magnetic grain size, due to dissolution of fine-grained magnetite (Fig. 2B). On the other hand, the low-field magnetic susceptibility (k_{LF}) and IRM records are less affected by the possible dissolution process as they are dominated by the coarser magnetic grain size fraction (Fig. 2A). Both hysteresis loop and IRM acquisition diagrams indicate saturation fields at ~100 mT with coercivities typical for magnetite (Fig. 3; e.g., Dunlop and Özdemir, 1997). According to the k_{ARM} versus k_{LF} diagram (King et al., 1983) magnetic grain size are compatible with the presence of magnetite in the ~0.1–5 μm size range (Fig. 4A), with a finer assemblage above 3 m: the interval used for PSV and RPI reconstructions. Similarly, the Mrs/Ms and Hcr/Hc ratios (where: Ms = saturation magnetization; Hc = coercive force; Mrs = saturation remanence; Hcr = coercivity of remanence) are typical for pseudo-single domain (PSD) magnetite according to the Day plot (Fig. 4B; Day et al., 1977).

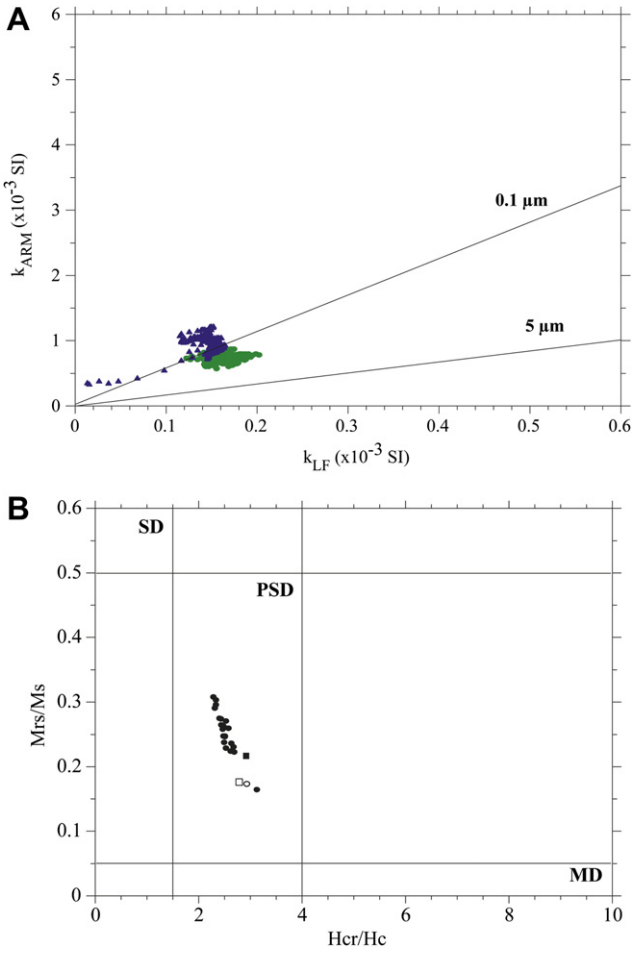

Fig. 4. (A) Magnetic grain size estimates. Blue triangles and green full circles symbols represent inferred grain size above and below 300 cm, respectively. Grain size contours are based on the measurement of synthetic magnetite samples by King et al. (1983). (B) Diagram of hysteresis ratios (Day plot) with single domain (SD), pseudo-single domain (PSD) and multi-domain (MD) regions for magnetite according to Day et al. (1977). The square and open symbols are associated to Fig. 3.

4.3. Natural remanent magnetization

The analysis of the vector end-point diagrams (Zijderveld, 1967) reveals the presence of two magnetic components (Fig. 5B): a low-coercivity component (viscous magnetization) in the 0–15 mT coercivity interval and a stable well-defined, characteristic magnetization. The latter was isolated by PCA analysis (Kirschvink, 1980) using 10 demagnetization steps between 20 and 80 mT. MAD values are well below 5° and the ChRM inclinations fluctuate around the expected inclination calculated according to the geocentric axial dipole (I_{GAD}) model at the coring site (80°) (Fig. 5A), indicating a well-preserved paleomagnetic signal. Moreover, the MDF_{NRM} and MDF_{ARM} vary around 35 mT and 30 mT respectively, whereas the MDF_{IRM} values are lower than the MDF_{ARM} values (Fig. 5A). These results indicate that the magnetic properties of Core 650 are mainly controlled by low-coercivity ferrimagnetic minerals such as magnetite (e.g., Dunlop and Özdemir, 1997).

If we focus on the top 240 cm (the interval used for the PSV and RPI reconstruction), only a single case of slight sediment disturbance is detected at the base of a u-channel at one of the section breaks (from 74 to 77 cm; Fig. 6). No deformation is observed at the top of the following u-channel (77–81 cm), nor

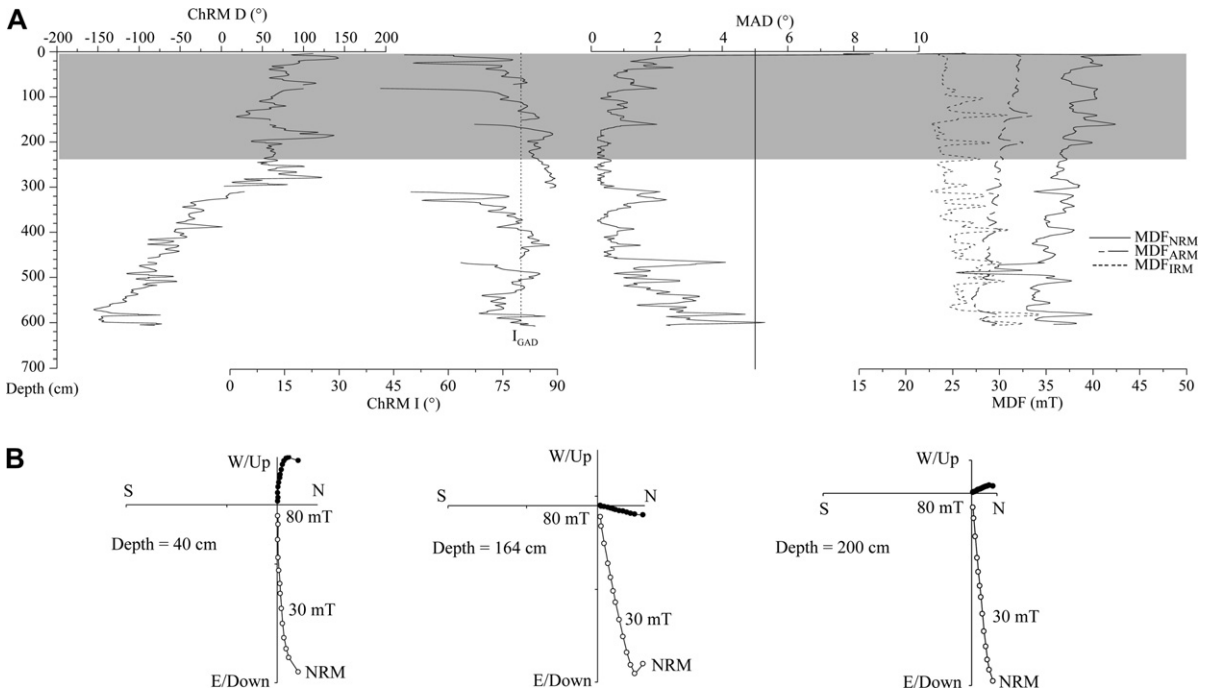

Fig. 5. The characteristic remanent magnetization (ChRM) of Core 650. (A) From left to right are displayed: the magnetic declination (D), inclination (I) of the ChRM as well as the corresponding MAD values and median destructive fields (MDF). Note that the ChRM D profiles are relative since the core was not azimuthally oriented. The broken vertical line in the ChRM inclination diagram represents the expected inclination (I_{GAD}) for a geocentric axial dipole model, whereas the solid vertical line indicates a MAD value of 5°. The gray shaded area indicates the interval used for PSV and RPI reconstructions. (B) Representative vector end-point orthogonal projection diagrams (Zijderveld, 1967) at three selected depths. AF demagnetization data reveal a stable single component magnetization that is directed toward the origin of the vector component diagram. Open (closed) symbols represent vector end points projected on the vertical (horizontal) plane, respectively. Peak alternating fields are indicated in millitesla.

at the other section break (from 153 to 160 cm; Fig. 6). In addition, no high MAD values were observed at the base or top of the u-channels (Figs. 5 and 6) in these two core breaks. In summary, even if possible dissolution may have occurred downcore, the sediments are characterized by well-defined, strong characteristic magnetization carried by PSD grains with a uniform grain size. In addition, all the magnetic parameters and hysteresis properties point to low-coercivity minerals, such as magnetite, as the main carriers of the magnetic remanence.

4.4. Relative paleointensity (RPI) determination

Estimation of relative paleointensity (RPI) from sediments can be obtained by normalizing the measured NRM by an appropriate magnetic parameter in order to compensate for the variable concentration of ferrimagnetic minerals (e.g., Tauxe, 1993). Concentration-dependent parameters such as ARM, IRM or k_{LF} are generally employed as normalizer. To assess the reliability of an RPI proxy some pre-established criteria must be satisfied. According to Tauxe (1993), the NRM must be characterized by a strong, stable, single component magnetization carried by (titano)magnetite in the 1–15 μm (SD/PSD) grain size range. Moreover, due to the effect of magnetostatic interaction between ferrimagnetic particles on the ARM acquisition (Sugiura, 1979) concentration of magnetite should not vary downcore by more than a factor of 10 (Tauxe, 1993). Finally, the normalized paleointensity records from the same geographical area should display similar pattern.

As shown in the previous sections, the ChRM of Core 650 is characterized by MAD values <5° carried by relatively uniform fine-grained magnetite (Fig. 4A and B). The ARM varies by less than a factor of 3 (Fig. 2A). However, as stated in the previous sections, the ARM profile likely reflects a slight downcore coarsening (Fig. 2A). In addition, below ~1 μm the ARM is strongly grain size dependent (e.g., Dunlop and Özdemir, 1997). Therefore, due to the small magnetic grains observed in Core 650 (Fig. 4A), the use of the ARM as a normalizer may not be appropriate. In contrast, both k_{LF} and IRM are not affected in the same way as the ARM (Fig. 2A) and are therefore likely more suitable for these sediments. This is well illustrated in Fig. 10 where NRM/IRM and NRM/k_{LF} yield similar results both in terms of fluctuation and amplitude, whereas NRM/ARM seems to capture a more pronounced long-term trend and lower amplitude fluctuations, especially from 2500 to 5000 cal BP. NRM/IRM and NRM/k_{LF} are also consistent with a previously published record from the Beaufort Sea (Core 803; Barletta et al., 2008; Fig. 10) and further support the use of k_{LF} or IRM as a normalizer.

4.5. Paleomagnetic dating of Core 650

A direct comparison ($R = 0.71$) of the relative ChRM declination of Core 650 and the computed declination from the CALS7k.2 model is possible for the first 240 cm and allows the detection of nine common paleomagnetic declination features during the last 6000 cal BP (Fig. 7). An age model was then constructed transferring these chronostratigraphic markers and the available AMS-^{14}C date on the first 240 cm of Core 650. A fifth-order polynomial fit ($R = 0.999$) was used between the uppermost and the lowermost dates (Fig. 8). With these assumptions, a mean sedimentation rate of ~33.4 cm/ka was estimated.

In order to verify the robustness of this approach, the derived ChRM inclination profile of Core 650 is compared with other high-resolution western North American Holocene PSV records. As revealed from Fig. 9, two distinctive magnetic inclination features at ~1800 and ~2500 cal BP (magnetic features I-1 and I-2,

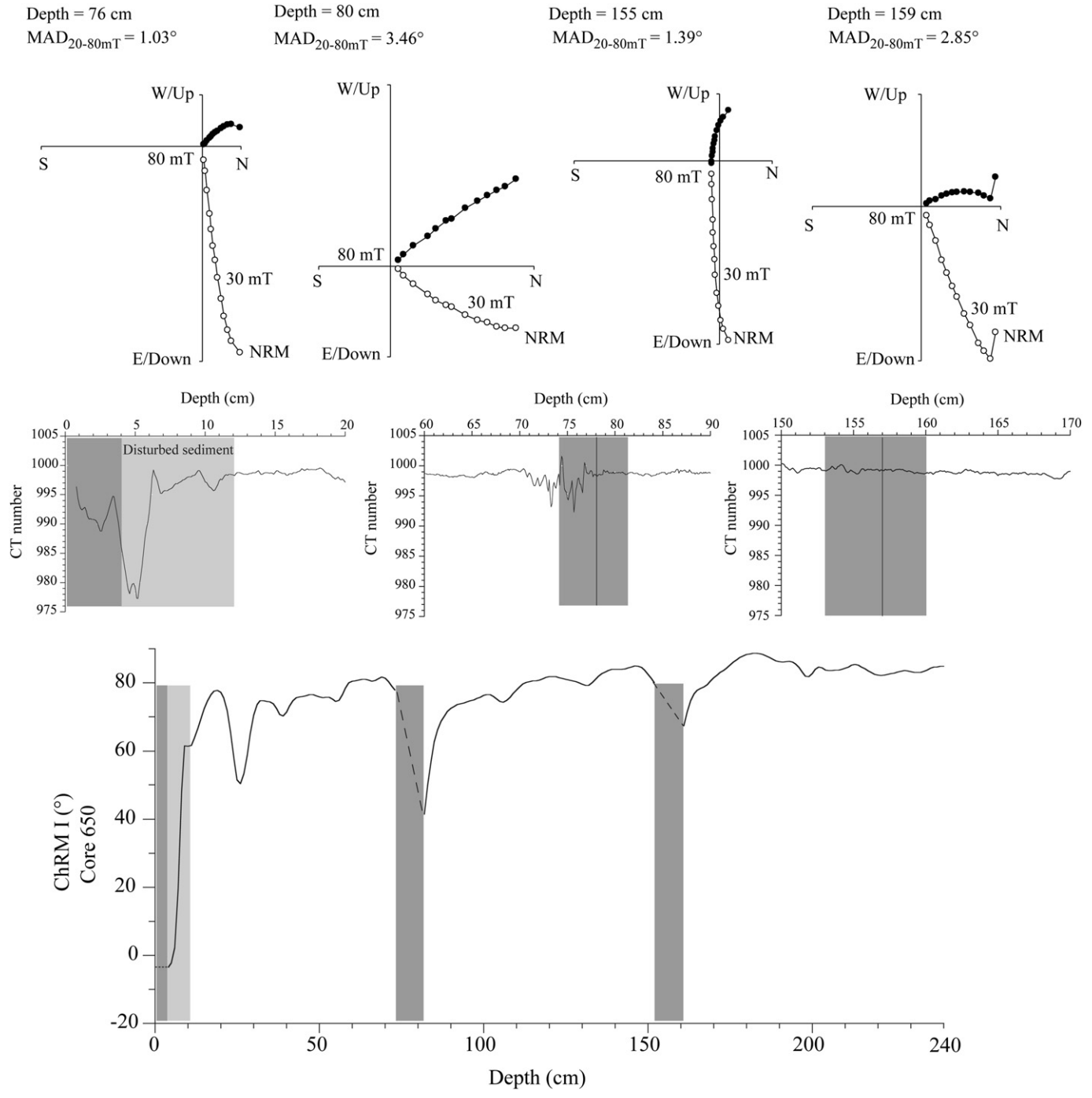

Fig. 6. Magnetic inclination record of Core 650 (first 240 cm; lower diagram) and the computerized tomography (CT) numbers derived from the CAT-scan (computerized axial tomography) analysis at the three core breaks (middle diagrams). Shaded dark-gray areas indicate the three intervals affected by an edge effect at core breaks due the response function of the cryogenic magnetometer (see text for details), whereas the vertical line represent the precise location of the section breaks. The paleomagnetic data in these three intervals (0–4 cm, 74–81 cm and 153–160 cm) were excluded, but note the homogenous nature of the CT number profiles from 77 cm and below, as well as from 153 cm and below, indicative of undisturbed sediments. On the contrary, major changes in the CT number profile of the first ~12 cm are indicative of a coring artefact. The vector end-point orthogonal projection diagrams (upper diagrams) below and above each section break associated with the magnetic features I-1 and I-5 (see Fig. 9) reveal high-quality component directions (MAD <5°). Closed (open) symbols represent projection on the horizontal (vertical) planes of the orthogonal projections.

respectively) are present in all the considered records as well as in the CALS7k.2 model. The different nature of the PSV records (marine: Cores 05 and 803 (Barletta et al., 2008); lacustrine: Mara Lake (Turner, 1987); volcanic rocks: paleomagnetic secular variation from lava flows (PSVL) compilation (Hagstrum and Champion, 2002)) further corroborates the geomagnetic origin of these signals. Moreover, three magnetic inclination minima (I-3 ~3000 cal BP; I-4 ~3700 cal BP; I-5 ~4600 cal BP; Fig. 9) are observed in all the marine sedimentary sequences from the Chukchi and Beaufort Seas. However, as depicted from Fig. 9, the inclination values of the magnetic features I-2 and I-5 overlap two core breaks. Even though the deleted data represent a cumulative 8 cm at core break, the

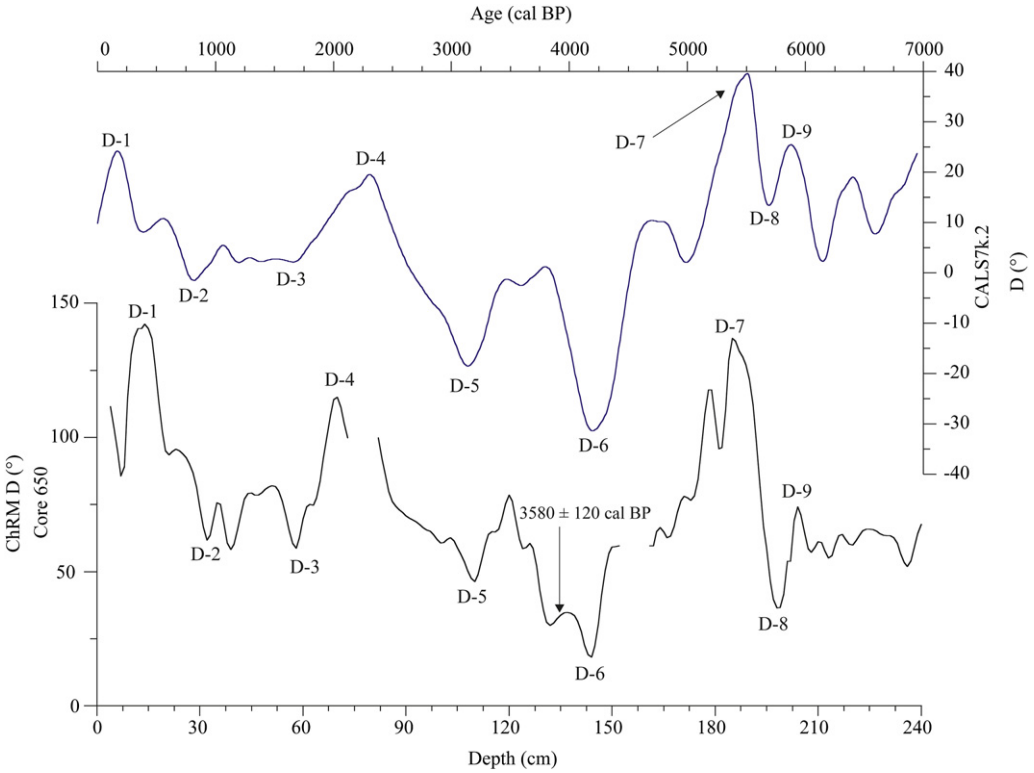

Fig. 7. The calculated magnetic declination (upper blue curve) from the CALS7k.2 model for the past 7000 cal BP (as expected for the Beaufort Sea region) and the relative ChRM declination curve of Core 650 versus depth (lower black curve). The proposed nine magnetic declination features (D-1 to D9) as well as the available AMS-^{14}C date used to construct the age model are indicated. Note that the declination scales are not identical.

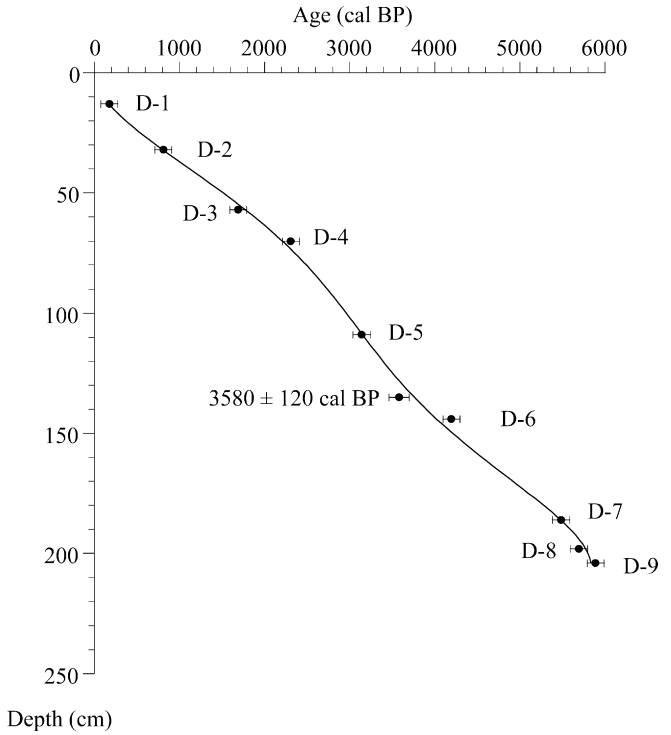

Fig. 8. Age model of Core 650. The age model was constructed using a fifth-order polynomial fit ($R = 0.999$) between the chronostratigraphic markers of Fig. 7 and the available AMS-^{14}C date of Core 650. Uncertainties associated with the magnetic declination features are assumed to be ~100 yr according to the temporal resolution of the CALS7k.2 model (Korte and Constable, 2005).

inclination minima I-2 and I-5 still reveal a clear trend reflected by several data points. Regardless of these two inclination minima and in addition to the inclination maxima, the overall correspondence between the inclination curves of the different records (Fig. 9) can be ascribed to variations in Earth's magnetic field.

The derived relative paleointensity record of Core 650 using both k_{LF} and IRM as normalizers (Fig. 10) depicts similar millennial-scale fluctuations when compared to other previously published RPI records from the same geographical area (Cores 05 and 803: Barletta et al., 2008; Core 06: Lisé-Pronovost et al., 2009; see Fig. 1 for location) further supporting the derived age model. Two RPI highs at ~2000 and 4000 cal BP are notably observed (P-1 and P-3; Fig. 10) and were previously recognised by Barletta et al. (2008) as two distinctive western Canadian Arctic chronostratigraphic markers.

5. Conclusion

In conclusion, our study reveals the potential of using the CALS7k.2 model as a relative dating tool in the Canadian Arctic. The actual North American database used to constrain the CALS7k.2 model seems sufficient to describe most of the millennial-scale Holocene PSV features observed in the western Canadian Arctic as previously highlighted by Barletta et al. (2008) and Lisé-Pronovost et al. (2009). Recently, Ledu et al. (in press) used similarities in the magnetic inclination record and the CALS7k.2 output to improve the age model of a Holocene marine sedimentary sequence collected from the Lancaster Sound (eastern Canadian Arctic). Accordingly, these results open the possibility of using this chronostratigraphic approach in both the western and eastern Canadian Arctic.

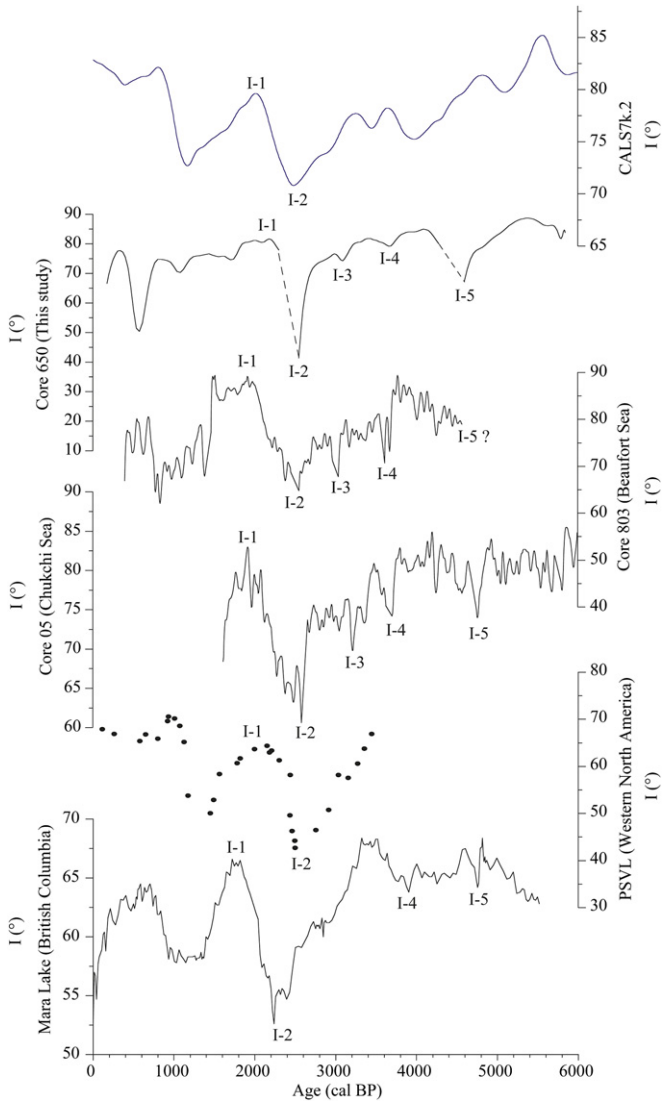

Fig. 9. Comparison of western North American magnetic inclination records for the past 6000 cal BP. Common magnetic inclination features are indicated. PSV records are from: Mara Lake, British Columbia, Canada (Turner, 1987); PSVL = paleomagnetic secular variation record from lava flows, Western North America, USA (Hagstrum and Champion, 2002); Cores 05 and 803 from the Chukchi and the Beaufort Seas, respectively (Barletta et al., 2008); Core 650, this study (note that the data along the u-channels section breaks are excluded because they are affected by an "edge effect" due to the response function of the cryogenic magnetometer). The magnetic inclination expected for the Beaufort Sea from the CALS7k.2 model is also displayed (blue upper curve). The original PSV record from Mara Lake was calibrated using the IntCal04 radiocarbon calibration curve (Reimer et al., 2004). Note that the magnetic inclination scales are not identical.

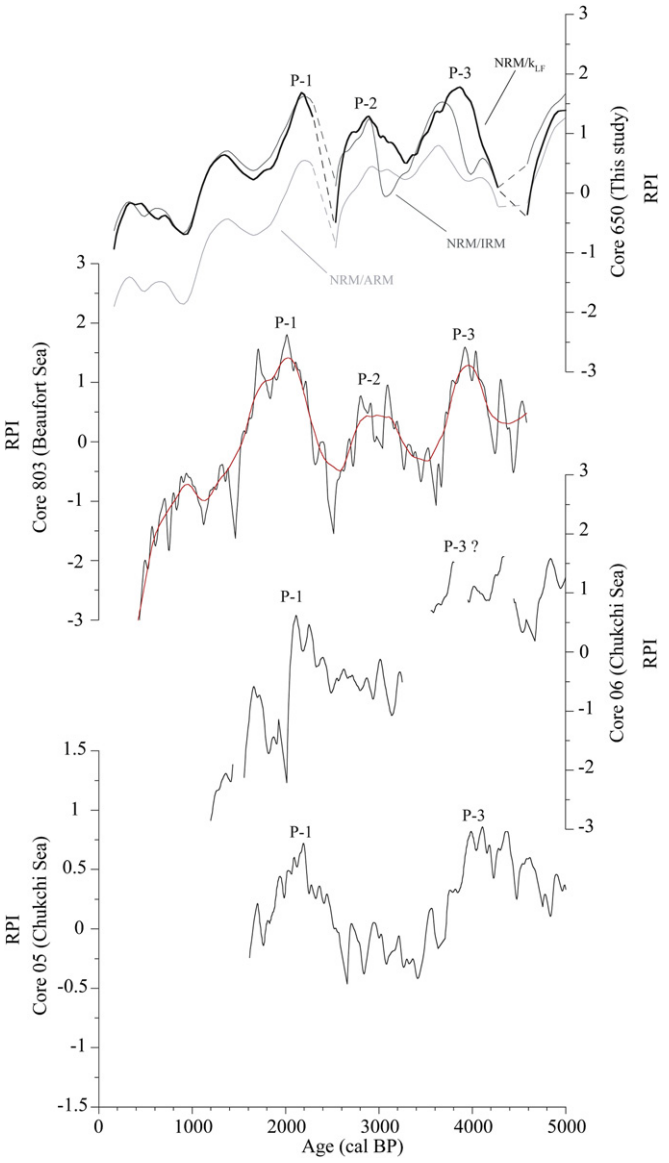

Fig. 10. Relative paleointensity (RPI) records of Cores 05 (Barletta et al., 2008), 06 (Lisé-Pronovost et al., 2009), 650 (this study) and 803 (Barletta et al., 2008) on their own chronologies. The RPI data of Core 650 were obtained by dividing the NRM after an AF demagnetization of 30 mT by the k_{LF} (thick black curve), ARM (light gray curve) and IRM (dark-gray curve), respectively. Note the similarities in both shape and amplitude of the derived RPI proxies of Core 650 using both k_{LF} and IRM as normalizer as well as the general agreement between the RPI record of Core 650 and the other RPI records. All the data are standardized according to their mean and standard deviation. The curve fit in the RPI record of Core 803 (red curve in the web version) was calculated by using the locally weighted least squares method with a 9% weighting function. Correlative paleointensity features are indicated (P-1 to P-3).

Acknowledgements

We are in debt to the captain, officers, crew and scientists on board the CCGS Amundsen for the recovery of Core 2004-804-650. We wish to thank the two anonymous reviewers for their constructive reviews as well as Dr. M. Korte for providing the CALS7k.2 model output for the Beaufort Sea. We thank Jacques Labrie for his technical support. This study was supported by the Canadian Arctic Shelf Exchange Study (CASES), NSERC Discovery and Northern supplement as well as Special Research Opportunity (IPY) grants to G.S. and A.R. This is GEOTOP contribution number 2010-0004.

References

Andrews, J.T., Dunhill, G., 2004. Early to mid-Holocene Atlantic water influx and deglacial meltwater events, Beaufort Sea slope, Arctic ocean. Quaternary Research 61, 14–21.

Barletta, F., St-Onge, G., Channell, J.E.T., Rochon, A., Polyak, L., Darby, D.A., 2008. High-resolution paleomagnetic secular variation and relative paleointensity records from the western Canadian Arctic: implication for Holocene stratigraphy and geomagnetic field behaviour. Canadian Journal of Earth Sciences 45, 1265–1281.

Blott, S.J., Pye, K., 2001. Gradistat: a grain size distribution and statistics package for the analysis of unconsolidated sediments. Earth Surface Processes and Landforms 26, 1237–1248.

Bringué, M., 2009. Paléocéanographie et variabilité climatique sur le talus du Mackenzie (Mer de Beaufort, Arctique canadien) au cours de l'Holocène. M.Sc. Thesis, Université du Québec à Rimouski, Rimouski, Canada, 104 pp.

Channell, J.E.T., Xuan, C., 2009. Self-reversal and apparent magnetic excursions in Arctic sediments. Earth and Planetary Science Letters 284, 124–131.
Darby, D.A., Polyak, L., Bauch, H.A., 2006. Past glacial and interglacial conditions in the Arctic ocean and marginal seas – a review. Progress in Oceanography 71, 129–144.
Darby, D.A., Polyak, L., Jakobsson, M., 2009. The 2005 HOTRAX Expedition to the Arctic ocean. Global and Planetary Change 68, 1–4.
Day, R., Fuller, M., Schmidt, V.A., 1977. Hysteresis properties of titano-magnetite: grain size and compositional dependence. Physics of the Earth and Planetary Interiors 13, 260–267.
Dumberry, M., Finlay, C.C., 2007. Eastward and westward drift of the Earth's magnetic field for the last three millennia. Earth and Planetary Science Letters 254, 146–157.
Dunlop, D.J., Özdemir, Ö, 1997. Rock Magnetism: Fundamentals and Frontiers. Cambridge University Press, Cambridge, New York.
Guyard, H., Chapron, E., St-Onge, G., Anselmetti, F., Arnaud, F., Magand, O., Francus, P., Mélières, M.-A., 2007. High-altitude varve records of abrupt environmental changes and mining activity over the last 4000 years in the Western French Alps (Lake Bramant, Grandes Rousses Massif). Quaternary Science Reviews 26, 2644–2660.
Hagstrum, J.T., Champion, D.E., 2002. A Holocene paleosecular variation record from 14C-dated volcanic rocks in western North America. Journal of Geophysical Research 107, 1–14.
Hillaire-Marcel, C., 2008. Decadal- to millennial-scale variability of Arctic-Subarctic oceans and adjacent lands: a contribution of the Polar Climate Stability Network of Canada to the International Polar Year. Canadian Journal of Earth Sciences 45, 1199–1201.
Hughen, K.A., Baillie, M.G.L., Bard, E., Bayliss, A., Beck, J.W., Bertrand, C.J.H., et al., 2004. Marine04 Marine radiocarbon age calibration, 0–26 Cal Kyr BP. Radiocarbon 46, 1059–1086.
Keigwin, L.D., Donnelly, J.P., Cook, M.S., Driscoll, N.W., Brigham-Grette, J., 2006. Rapid sea-level rise and Holocene climate in the Chukchi Sea. Geology 34, 861–864.
King, J.W., Banerjee, S.K., Marvin, J., 1983. A new rock-magnetic approach to selecting sediments for geomagnetic paleointensity studies: application to paleointensity for the last 4000 years. Journal of Geophysical Research 88, 5911–5921.
Kirschvink, J.L., 1980. The least-squares line and plane and the analysis of paleomagnetic data. Geophysical Journal of the Royal Astronomical Society 62, 699–718.
Korte, M., Constable, C.G., 2005. Continuous geomagnetic field models for the past 7 millennia: 2. CALS7K. Geochemistry, Geophysics, Geosystems 6 (Q02H16). doi:10.1029/2004GC000801.
Korte, M., Genevey, A., Constable, C.-G., Frank, U., Schnepp, E., 2005. Continuous geomagnetic field models for the past 7 millennia: 1. A new global data compilation. Geochemistry, Geophysics, Geosystems 6 (Q02H15). doi:10.1029/2004GC000800.
Korte, M., Mandea, M., 2008. Magnetic poles and dipole tilt variation over the past decades to millennia. Earth Planets and Space 60, 937–948.
Ledu, D., Rochon, A., de Vernal, A., St-Onge, G., 2008. Palynological evidence of Holocene climate oscillations in the Eastern Arctic: a possible shift in the Arctic oscillation at the millennial time scale. Canadian Journal of Earth Sciences 45, 1363–1375.
Ledu, D., Rochon, A., de Vernal, A., St-Onge, G. Holocene paleoceanography of the Northwest Passage, Canadian Arctic Archipelago: the possible onset of an Arctic oscillation climate mode. Quaternary Science Reviews, in press.
Lisé-Pronovost, A., St-Onge, G., Brachfeld, S., Barletta, F., Darby, D., 2009. Paleomagnetic constraints on the Holocene stratigraphy of the Arctic Alaskan margin. Global and Planetary Change 68 (1–2), 85–99.
Mazaud, A., 2005. User-friendly software for vector analysis of the magnetization of long sediment cores. Geochemistry, Geophysics, Geosystems 6. doi:10.1029/2005GC001036.
McKay, J.L., de Vernal, A., Hillaire-Marcel, C., Not, C., Polyak, L., Darby, D., 2008. Holocene fluctuations in Arctic sea-ice cover: dinocyst-based reconstructions for the eastern Chukchi Sea. Canadian Journal of Earth Sciences 45, 1377–1397.
McNeely, R., Dyke, A.S., Southon, J.R., 2006. Canadian Marine Reservoir Ages, Preliminary Data Assessment. Open File 5049. Geological Survey Canada, Ottawa.
Newitt, L.R., Mandea, M., McKee, L.A., Orgeval, J.-J., 2002. Recent acceleration of the north magnetic pole linked to magnetic jerks. Eos, Transactions, American Geophysical Union 83 (35), 381–389.
Peters, C., Thompson, R., 1998. Magnetic identification of selected natural iron oxides and sulfides. Journal of Magnetism and Magnetic Materials 183, 365–374.
Polyak, L., Bischof, J., Ortiz, J.D., Darby, D.A., Channell, J.E.T., Xuan, C., Kaufman, D.S., Løvlie, R., Schneider, D., Adler, R., Council, E., 2009. Late Quaternary stratigraphy and sedimentation patterns in the western Arctic Ocean. Global and Planetary Change 68, 5–17.
Reimer, P.J., Baillie, M.G.L., Bard, E., Bayliss, A., Beck, J.W., Bertrand, C., Blackwell, P.G., Buck, C.E., Burr, G., Cutler, K.B., Damon, P.E., Edwards, R.L., Fairbanks, R.G., Friedrich, M., Guilderson, T.P., Hughen, K.A., Kromer, B., McCormac, F.G., Manning, S., BronkRamsey, C., Reimer, R.W., Remmele, S., Southon, J.R., Stuiver, M., Talamo, S., Taylor, F.W., van der Plicht, J., Weyhenmeyer, C.E., 2004. IntCal04 atmospheric radiocarbon age calibration, 26–0 ka BP. Radiocarbon 46, 1026–1058.
Rochon, A., Scott, D.B., Schell, T.M., Blasco, S., Bennett, R., Mudie, P.J., 2006. Evolution of sea surface conditions during the Holocene: comparison between Eastern (Baffin Bay and Hudson Strait) and Western (Beaufort Sea) Canadian Arctic. Eos, Transactions, American Geophysical Union 87 (52) Fall Meet. Suppl. Abstract U43B-0867.
Sagnotti, L., Rochette, P., Jackson, M., Vadeboin, F., Dinarès-Turell, J., Winkler, A., "Mag-Net" Science Team, 2003. Inter-laboratory calibration of low-field magnetic and anhysteretic susceptibility measurements. Physics of the Earth and Planetary Interiors 138, 25–38.
Stoner, J.S., St-Onge, G., 2007. Magnetic stratigraphy in paleoceanography: reversals, excursions, paleointensity and secular variation. In: Hillaire-Marcel, C., de Vernal, A. (Eds.), Proxies in Late Cenozoic Paleoceanography. Elsevier, pp. 99–137.
St-Onge, G., Mulder, T., Francus, P., Long, B., 2007. Continuous physical properties of cored marine sediments. Developments in Marine Geology 1. doi:10.1016/S1572-5480(07)01007-X.
St-Onge, G., Stoner, J.S., Hillaire-Marcel, C., 2003. Holocene paleomagnetic records from the St. Lawrence Estuary: centennial- to millennial-scale geomagnetic modulation of cosmogenic isotopes. Earth and Planetary Science Letters 209, 113–130.
Stuiver, M., Polach, H.A., 1977. Discussion: reporting of 14C data. Radiocarbon 19, 355–363.
Stuiver, M., Reimer, P.J., Reimer, R.W., 2005. CALIB 5.0 Available from: http://radiocarbon.pa.qub.ac.uk/calib/.
Sugiura, N., 1979. ARM, TRM, and magnetic interactions: concentration dependence. Earth and Planetary Science Letters 42, 451–455.
Tauxe, L., 1993. Sedimentary records of relative paleointensity: theory and practice. Reviews of Geophysics 31, 319–354.
Turner, G.M., 1987. A 5000 year geomagnetic paleosecular variation record from western Canada. Geophysical Journal International 91 (1), 103–121.
Weeks, R., Laj, C., Endignoux, L., Fuller, M., Roberts, A., Manganne, R., Blanchard, E., Goree, W., 1993. Improvements in long-core measurement techniques: applications in palaeomagnetism and palaeoceanography. Geophysical Journal International 114, 651–662.
Xuan, C., Channell, J.E.T., 2010. Origin of apparent magnetic excursions in deep-sea sediments from Mendeleev–Alpha Ridge, Arctic ocean. Geochemistry, Geophysics, Geosystems 11 (Q02003). doi:10.1029/2009GC002879.
Zijderveld, J.D.A., 1967. AC demagnetization of rock: analysis of results. In: Collinson, D.W., Creer, K.M., Runcorn, S.K. (Eds.), Methods in Paleomagnetism. Elsevier, Amsterdam, pp. 254–286.